COMPDYN 2011
3rd ECCOMAS Thematic Conference on
Computational Methods in Structural Dynamics and Earthquake Engineering
M. Papadrakakis, M. Fragiadakis, V. Plevris (eds.)
Corfu, Greece, 25–28 May 2011

INFLUENCE OF THE FLUID-STRUCTURE INTERACTION ON THE MODAL ANALYSIS, AND ON THE DYNAMICS OF COMPOSITE MONOFIN : OPTIMIZATION OF PROPULSION

B. Mahiou, F. Razafimahery and L. R. Rakotomanana

IRMAR, UMR 6625, CNRS & Université de Rennes 1, Equipe de Mécanique
Campus de Beaulieu, 35042, Rennes Cédex
Email : benjamin.mahiou@free.fr
Email : fulgence.razafimahery@univ-rennes1.fr
Email : lalaonirina.rakotomanana-ravelonarivo@univ-rennes1.fr

Keywords: Fluid-structure interaction, modal analysis, thrust, finite element method.

Abstract. *This study aims to analyze the propulsive efficiency of a swimming multi-layers fin. For this purpose, we develop a finite element model accounting for the fluid-structure interaction and the structural anisotropy of each layer. Two types of fins have been tested by comparing their eigenfrequencies. A dynamical situation has been simulated by imposing a translation (heaving) and a rotation (pitching) motions at the end of the fin, using in some sense a relative frame attached to the ankle joint. Thrust, lift and pitching moment are evaluated and compared for the two types of fins.*

1 INTRODUCTION

The aquatic locomotion of animal constitutes a fascinating research domain in biomechanics. The search for performance of aquatic propulsion generated by a foil undergoing harmonic flapping, including translation (heaving) and rotation (pitching) motions, has stimulated numerous works during these last years e.g. [4], [10], [13], [17] . In the case of swimming with fins, the propulsive efficiency depends on several factors. Most previous models evaluate the dynamic performances, including drag and lift which are the two parameters usually considered as relevant to quantify the propulsive efficiency of a fin e.g. [12]. Some models are essentially of discrete type[11], [8], while others, inspired from propulsion of marine cetaceans, use continuous models [1], [18]. Most of these authors do not always demonstrate the highly coupled nature of the problem. In fact, for range of stresses observed in actual swimming, the coupling between the fluid and the fin cannot be neglected. Another aspect is the accounting of the ankle muscle for the propulsion. The frequency determination is deemed necessary since the muscle activity during fin swimming has important correlation with the oscillating flapping frequency e.g. [9]. The activation of muscles increases up to $25\ \%$ when the swimming frequency increases from $0.8\ [Hz]$ to $1\ [Hz]$. In order to improve the adequation of fin with muscle activities, previous studies highlight the role of structural composites and their arrangement for optimizing the propulsion of fin. The static deformation together with the eigenfrequencies of the fin are considered as basic parameters for optimization e.g. [7]. Unfortunately most of them do not account for the water interaction with the fin.

This work is mainly numerical and develops a continuous model in the framework of the fluid-structure interaction approach and constitutes a continuation of a previous study in [2]. The goal is to undertake a parametric analysis of two different designs of multi-layers fin by comparing their eigenfrequencies by accounting for the water interaction. We simulate the evolution of thrust and lift forces, together with the moment (torque about the pitch axis) during a steady propulsion. This approach enables a parametric study, where we can vary some data related to the geometrical, physical and kinematic model. The study consists of three parts. The first part sets out the different assumptions underlying, the development of the theoretical basic model. In the second part, we focus on the modal analysis. To this end, we analyze the changes of eigenfrequencies when varying the physical characteristics of the fin. We are interested on the influence of the layers arrangement and on the influence of the interacting water on the fin eigenmodes. The third part deals with the dynamics. For this purpose, we consider a frame attached to the fin, or more precisely at the foot of the swimmer, and impose a translational (heaving) and rotational (pitching) motions. Two types of multi-layers fins are also studied.

2 Theoretical model of the multi-layers fin

We assume an amateur swimmer, where the range of velocity U_0 is assumed to be small compared to the compression wave celerity c_L within the material of the fin. The ratio $\varepsilon = U_0/c_L << 1$, called displacement parameter, allows to characterize the nature of the coupling considered in this work. It has been shown in [3] that the adapted model is the inertial coupling.

The model is bidimensional (since we are mainly interested in the first bending modes in this preliminary analysis) and the (thin) fin is immersed in a large swimming pool. The fin is modeled by a multilayer linear elastic transverse anisotropic material. The fluid domain is denoted Ω_f, while each layer constituting the fin is denoted by Ω_i and has the density ρ_i.

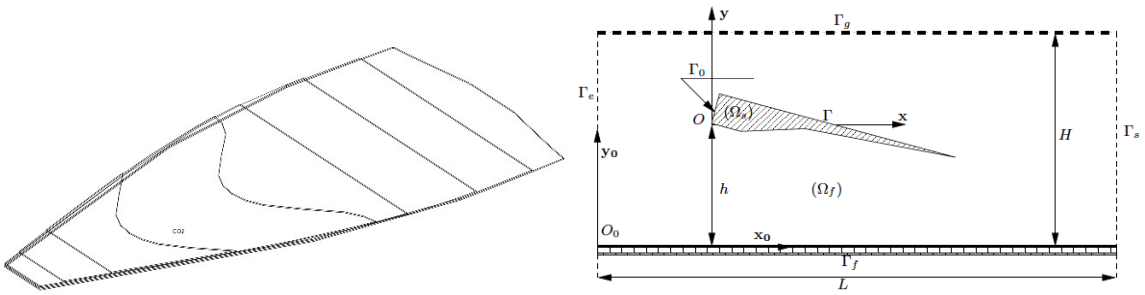

Figure 1: Geometry of 3D fin (dimensions are given below) and scheme of the computational domain (Dimensions of the swimming pool : length 5 $[m]$, depth 2 $[m]$).

2.1 Basic equations

We denote $\mathbf{u}_i$ the displacement field in the fin and p the pressure field in the water, which is considered as non viscous compressible fluid. The quantities c_0 and ρ_0 denote the sound velocity and density of the water respectively. We accordingly remain in the framework of vibro-acoustic problems. The longitudinal axis of the fin is denoted $\mathbf{x}$. Use of the ALE method is not necessary in this study because the material is assumed linear and the deformation is assumed small. In the frame attached to the fin, the problem is to find $(\mathbf{u}_i, p)$ solutions

$$\left\{\begin{array}{rcll} \rho_i \dfrac{\partial^2 \mathbf{u}_i}{\partial t^2} & = & \nabla \cdot \sigma(\mathbf{u}_i) + \rho_i \mathbf{F} & (\Omega_i) \\ \dfrac{1}{\rho_0 c_0^2} \dfrac{\partial^2 p}{\partial t^2} & = & \nabla \cdot \left[\dfrac{1}{\rho_0} \left(\nabla p - \rho_0 \mathbf{F} \right) \right] & (\Omega_f) \\ \mathbf{u} & = & \mathbf{0} & (\Gamma_0) \\ \sigma(\mathbf{u})\mathbf{n} & = & -p\mathbf{n} & (\Gamma) \\ [\nabla p - \mathbf{q}] \cdot \mathbf{n} & = & -\rho_0 \dfrac{\partial^2 \mathbf{u}}{\partial t^2} \cdot \mathbf{n} & (\Gamma) \\ [\nabla p - \mathbf{q}] \cdot \mathbf{n} & = & 0 & (\Gamma_1) \\ p & = & 0 & (\Gamma_L) \\ \sigma(\mathbf{u}_i) & = & \mathbb{K}(\theta_i)\varepsilon(\mathbf{u}_i) & (\Omega_i) \end{array}\right. \tag{1}$$

where $\mathbf{F}$ is the relative and Coriolis force induced by the heaving and pitching motions (relative frame concept) of the fin. The angle θ_i denotes the orientation of fibers relative to the longitudinal axis $\mathbf{x}$ on the fin. In our case, each layer is made of matrix and carbon fibers. The orientation of fibers is usually $0°$ or $90°$ relative to the axis of the fin. The physical properties of each layer defined by the tangent stiffness $\mathbb{K}(\theta_i)$ are well defined for anisotropic componenet e.g. [14]. However, some characteristic values are not displayed for industrial confidentiality reason. In this study, each layer has the same properties, only the fiber orientation is different for each layer as indicated below.

2.2 Modal analysis of coupled problem

For the modal analysis, we search for the eigenfrequencies and modal shapes of the fin in vacuum and in water. Indeed, to test the quality of a fin, it is usual to determine its quasi-static deformed shape and dynamic response in air (approximately as in vacuum). The objective here is to test if the presence of the surrounding fluid can or cannot be quantitavely neglected. The frequencies provide key information for the dynamic behavior of the fin e.g. [8]. The modal problem associated with the system (1) is to find the displacement, the pressure and the

eigenfrequencies $(\mathbf{u}_i, p, \omega)$ solutions

$$\left\{\begin{array}{rcll} -\rho_i\omega^2\mathbf{u}_i & = & \nabla\cdot\sigma(\mathbf{u}_i) & (\Omega_i) \\ -\dfrac{p}{\rho_0 c_0^2}\omega^2 & = & \nabla\cdot\left[\dfrac{1}{\rho_0}\nabla p\right] & (\Omega_f) \\ \mathbf{u} & = & \mathbf{0} & (\Gamma_0) \\ \sigma(\mathbf{u})\mathbf{n} & = & -p\mathbf{n} & (\Gamma) \\ \nabla p\cdot\mathbf{n} & = & \rho_0\omega^2\mathbf{u}\cdot\mathbf{n} & (\Gamma) \\ \nabla p\cdot\mathbf{n} & = & 0 & (\Gamma_1) \\ p & = & 0 & (\Gamma_L) \\ \sigma(\mathbf{u}_i) & = & \mathbb{K}(\theta_i)\varepsilon(\mathbf{u}_i) & (\Omega_i) \end{array}\right. \tag{2}$$

By introducing the spaces of test functions $\mathbf{V} = \{\mathbf{v}\in\mathbf{H}^1(\Omega_1),\ \mathbf{v}=\mathbf{0}\ (\Gamma_0)\}$ for displacement and $Q = H^1(\Omega)$ for pressure, the variational formulation of boundary value problem (2) holds

$$\left\{\begin{array}{rcl} \dfrac{d^2}{dt^2}\displaystyle\int_{\Omega_s}\rho\mathbf{u}\cdot\mathbf{v}dx + \int_{\Omega_s}\sigma(\mathbf{u}):\varepsilon(\mathbf{v})dx + \int_{\Gamma_1}p\mathbf{v}\cdot\mathbf{n}d\Gamma & = & 0 \\ \dfrac{d^2}{dt^2}\left(\displaystyle\int_{\Omega_f}\frac{p\phi}{\rho_0 c_0^2}dx + \int_{\Gamma_1}\mathbf{u}\cdot\mathbf{n}\phi d\Gamma\right) + \int_{\Omega_f}\frac{1}{\rho_0}\nabla p\cdot\nabla\phi dx & = & 0 \end{array}\right. \quad \forall(\mathbf{v},\phi)\in\mathbf{V}\times Q \tag{3}$$

with $\displaystyle\int_{\Omega_s}\rho\mathbf{u}\cdot\mathbf{v}dx = \sum_{i=1}^{N_L}\int_{\Omega_i}\rho_i\mathbf{u}_i\cdot\mathbf{v}_i dx$ and $\displaystyle\int_{\Omega_s}\sigma(\mathbf{u}):\varepsilon(\mathbf{v})dx = \sum_{i=1}^{N_L}\int_{\Omega_i}\sigma(\mathbf{u}_i):\varepsilon(\mathbf{v}_i)dx$, where N_L is a number of layers. Using Lagrange finite elements, where $\mathbf{u}_h\in\mathbb{P}_2\times\mathbb{P}_2$ and $p_h\in\mathbb{P}_1$, discretization of the variational problem (3) leads to the system

$$\left\{\begin{bmatrix}\mathbb{K}_1 & \mathbb{B}_1\\ \mathbb{O} & \mathbb{K}_p\end{bmatrix} - \omega^2\begin{bmatrix}\mathbb{M}_1 & \mathbb{O}\\ \mathbb{M}_{1a} & \mathbb{M}_p\end{bmatrix}\right\}\mathbf{X} = \mathbf{0} \tag{4}$$

This non symetric system is solved using the commercial software Comsol Multiphysics. Two types of calculations were carried out. The first is when the fin is plunged into a vacuum and the second interacting with water. We give below the results for a model up to five layers ($N_L = 5$) and the eigenfrequencies in vacuum (V) and in the water (W).

3 Numerical results

Two designs of multi-layers fins are compared in this section. Both of them are analyzed first in a vacuum and second in the swimming pool, and then interacting with water. Each layer is a biphasic composite and the matrix (m) and fiber (f) have the following properties respectively: Volume fraction $V_m = 0.4$ and $V_f = 0.6$, Young's modulus : $E_m = 3.45E9[GPa]$, and $38E9[GPa]$; Density $\rho_m = 1200[kg/m^3]$, and $\rho_f = 1950[kg/m^3]$; Poisson's ratio : $\nu_m = 0.3$, and $\nu_f = 0.22$.

3.1 Fin with Oriented fibers : $0°/90°/0°/90°/0°$

The fibers of each layer are arranged alternately along the two directions orthogonal axis **x** and **y** of the mean plane of the fin.

For this first fin, the first layer is oriented along **x**. The length of each layer is not the same. Lengths of layers are respectively $\ell := \ell_1 = 0.8[m]$, $\ell_2 = 0.6[m]$, $\ell_3 = 0.5[m]$, $\ell_4 = 0.4[m]$, and $\ell_5 = 0.3[m]$. Layer's length corresponds to the ply drop in [7]. The total thickness of the fin is maintained constant $e = 5.8[mm]$, and it is not depending on the number of layers. The fin is clamped at the end $x = 0$ and free of stress at end $x = \ell$.

1. Eigenfrequencies of fin in the vacuum

   The three-layers fin presents the highest eigenfrequencies in either a vacuum or in the water (see table 1), at least for the first frequencies.

	f_1	f_2	f_3	f_4	f_5	f_6	f_7	f_8
$2L$(V)	12.62	76.02	205.33	389.27	628.95	929.39	1293.32	1717.79
$3L$(V)	29.38	122.99	265.07	555.85	825.17	1326.14	1764.36	2321.13
$4L$(V)	22.68	90.16	192.04	404.72	600.38	958.85	1303.21	1692.38
$5L$(V)	28.82	79.74	185.16	373.97	560.99	904.69	1185.87	1632.83

Table 1: Eigenfrequencies f_n $[Hz]$ of the multi-layers fin in vacuum. Row $2L$ up to $5L$ indicates the number of layers of the fin.

2. Eigenfrequencies of fin interacting with water

	f_1	f_2	f_3	f_4	f_5	f_6	f_7	f_8
$2L$(W)	1.71	46.06	103.15	180.88	186.73	232.08	297.77	342.08
$3L$(W)	3.52	21.72	55.17	136.63	181.29	222.63	232.10	341.95
$4L$(W)	2.42	14.56	37.35	92.22	150.82	181.27	232.08	263.14
$5L$(W)	2.77	11.85	33.49	78.53	128.93	181.22	227.74	232.11

Table 2: Eigenfrequencies f_n $[Hz]$ of the multi-layers fin interacting with water. Row $2L$ up to $5L$ indicates the number of layers of the fin.

The fundamental eigenfrequency f_1 (and the others) depends on the arrangement of the layers. The two-layers fin has mostly the lowest fundamental frequency either in the vaccum or in the water (see table 2). There is systematically a peak of frequencies for the three-layers fin, not depending on the environnement (vacuum or water). This means that this arrangement induces the stiffest fin, at least for a dynamics point of view. The fundamental eigenfrequency of the coupled fin-water is far lower than of the fin in vacuum. This observation does not depend on the number of layers. To give an idea of the eigenmodes, we display on figure 2 the first six modal shapes of the fin interacting with the water for a five-layers case ($5L(W)$).

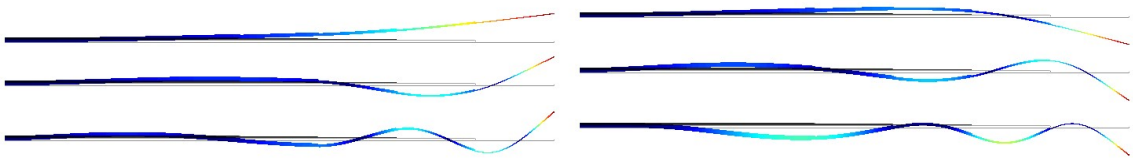

Figure 2: The first six mode shapes of the five-layers fin ($5L(W)$).

These are mainly bending modes for this 2D model. Due to the clamping at $x = 0$, and due to the progressive ply drop, the largest deformation is mainly located at the free end of the fin. For the terminolgy, if the first and second modes are involved for the propulsion, the fin swimming could be considered as undulatory type (anguilliform), whereas if the higher mode ranks are involved (oscillation of posterior part of the fin) then the fin swimming could be considered as carangiform e.g. [17].

3.2 Fin with Oriented fibers : $90°/0°/90°/0°/90°$

As for previous fin, fibers of each layer are arranged alternately along the two directions orthogonal axis **x** and **y** of the mean plane of the fin. However for this second fin, the first layer is oriented along $\mathbf{y}$. The length of each layer is not the same. Lengths of layers are respectively $\ell := \ell_1 = 0.8[m]$, $\ell_2 = 0.6[m]$, $\ell_3 = 0.5[m]$, $\ell_4 = 0.4[m]$, and $\ell_5 = 0.3[m]$. The total thickness of the fin is also maintained constant $e = 5.8[mm]$, and it is not depending on the number of layers. The fin is also clamped at the end $x = 0$ and free of stress at $x = \ell$.

1. Eigenfreqncies of fin in a vacuum

	f_1	f_2	f_3	f_4	f_5	f_6	f_7	f_8
$2L$(V)	12.61	73.51	158.46	273.94	488.33	757.90	997.37	1284.11
$3L$(V)	9.52	51.39	105.50	186.01	327.05	507.18	670.71	861.59
$4L$(V)	21.21	56.23	115.59	237.62	395.78	560.89	773.54	1093.47
$5L$(V)	17.44	44.84	91.62	186.19	313.60	444.60	606.69	867.88

Table 3: Eigenfrequencies f_n $[Hz]$ of the multi-layers fin in the vacuum. Row $2L$ up to $5L$ indicates the number of layers of the fin.

2. Eigenfrequencies of fin interacting with water

	f_1	f_2	f_3	f_4	f_5	f_6	f_7	f_8
$2L$(W)	1.71	13.30	39.45	72.24	136.51	181.24	232.04	235.54
$3L$(W)	1.14	8.74	23.87	45.06	86.89	147.57	181.24	215.08
$4L$(W)	2.28	9.53	23.83	50.30	97.46	156.71	181.22	219.41
$5L$(W)	1.68	6.89	17.23	36.93	70.87	113.85	161.15	181.31

Table 4: Eigenfrequencies f_n $[Hz]$ of the multi-layers fin interacting with water. Row $2L$ up to $5L$ indicates the number of layers of the fin.

Contrarily to the first type, the three-layers fin presents the lowest eigenfrequencies, and it is depending neither on the environnement vacuum or water, nor on the mode rank. Highest eigenfrequencies mostly correspond to the two-layers fin. Again, the influence of the fin-water interaction is pointed out, the presence of water, which is more realistic, in the model drastically decreases the eigenfrequencies of the fin.

Comparing the two types of multi-layers fins, we may observe that : the eigenfrequencies value depends strongly on the arrangement of layers, and such is the case either in a vacuum or in water. Fibers of the first layer along $\mathbf{x}$ seems to give highest fundamental eigenfrequency when there are several layers in the fin. The frequencies of the coupled model are always lower. It is quite understandable due to the effect of added mass from water interaction. Anticipating a study in progress in our team, it should also be observed that accounting the 3D effects decreased the fundamental frequency, which also corresponds to a bending modes, for instance the four-layers fin gives in vacuum $f_1 \simeq 7.74\ [Hz]$, and in water $f_1 \simeq 1.13\ [Hz]$ as fundamental eigenfrequency.

4 The dynamic problem

The dynamic problem was conducted using data in [15]. For this purpose, the fin is immersed in water, and is subjected to a combined heaving and pitching motions, mimicking the ankle joint motion. This motion is imposed at the end $x = 0$, the other end $x = \ell$ remains free. In this case, the force $\mathbf{F}$ induced by the relative frame motion introduced in the equation (1) has the expression :

$$\mathbf{F}(t) = -\begin{bmatrix} \ddot{h}(t)\sin[\omega(t)] - y\ddot{\omega}(t) - x\dot{\omega}^2(t) \\ \ddot{h}(t)\cos[\omega(t)] + x\ddot{\omega}(t) - y\dot{\omega}^2(t) \end{bmatrix} \tag{5}$$

in which we have defined the imposed translation and rotation e.g. [15] :

$$\begin{cases} \omega(t) = \theta_0 \sin(2\pi f t)\ ;\ h(t) = h_0 \sin(2\pi f t - \psi) \\ \theta_0 = 40^\circ\ ;\ \psi = \dfrac{\pi}{2}\ ;\ h_0 = 1c\ ;\ f = 0.225Hz \end{cases} \tag{6}$$

where $c = 0.7$ is the chord of the profile, that is to say, the length of the fin. The phase ψ is introduced to model the muscle dissymmetry. To avoid a resonance phenomenon, the excitation frequency is imposed small enough compared to the first natural frequency of the coupled system. The most relevant hydrodynamic parameters are the total force $\mathbf{R}$ and moment $\mathbf{M}$ exerted on the fin during the movement. Notice that these forces and moment are solely due to the water reaction. These quantities are defined by

$$\mathbf{R} = \int_\Gamma \sigma(\mathbf{u})\mathbf{n}d\Gamma\ ;\ \mathbf{M} = \int_\Gamma \mathbf{OM} \wedge \sigma(\mathbf{u})\mathbf{n}d\Gamma \tag{7}$$

The two components of D and L onto the axes $\mathbf{x}$ and $\mathbf{y}$, are respectively the drag and lift of the fin. The quantity $T(t) = -X(t)$ is called thrust. Different types of layers exist in the manufacture of fins, where the thickness is mostly fixed in advance. We test the same fins as in the modal analysis. Using the same notation as before, the variational formulation of boundary value problem (1) is then written

$$\begin{cases} \dfrac{d^2}{dt^2}\displaystyle\int_{\Omega_s} \rho\mathbf{u}\cdot\mathbf{v}dx + \int_{\Omega_s} \sigma(\mathbf{u}) : \varepsilon(\mathbf{v})dx + \int_{\Gamma_1} p\mathbf{v}\cdot\mathbf{n}d\Gamma &=& -\displaystyle\int_{\Omega_s} \rho\mathbf{F}\cdot\mathbf{v}dx \\ \dfrac{d^2}{dt^2}\left(\displaystyle\int_{\Omega_f} \frac{p\phi}{\rho_0 c_0^2}dx + \int_{\Gamma_1} \mathbf{u}\cdot\mathbf{n}\phi d\Gamma\right) + \displaystyle\int_{\Omega_f} \frac{1}{\rho_0}\nabla p\cdot\nabla\phi dx &=& \displaystyle\int_{\Omega_f} \frac{1}{\rho_0}\mathbf{q}\cdot\nabla\phi dx \end{cases} \tag{8}$$

forall $(\mathbf{v}, \phi) \in \mathbf{V} \times Q$, with $\mathbf{V} = \{\mathbf{v} \in \mathbf{H}^1(\Omega_1),\ \mathbf{v} = \mathbf{0}\ (\Gamma_0)\}$ and $Q = H^1(\Omega)$.

Using Lagrange finite elements, where $\mathbf{u}_h \in \mathbb{P}_2 \times \mathbb{P}_2$ et $p_h \in \mathbb{P}_1$, discretization of the variational problem (8) leads to the semi-discretized system

$$\begin{bmatrix} \mathbb{M}_1 & \mathbb{O} \\ \mathbb{M}_{1a} & \mathbb{M}_p \end{bmatrix} \frac{d^2\mathbf{X}}{dt^2} + \begin{bmatrix} \mathbb{K}_1 & \mathbb{B}_1 \\ \mathbb{O} & \mathbb{K}_p \end{bmatrix} \mathbf{X} = \mathbf{F} \tag{9}$$

with $\mathbf{X} = [\mathbf{U}, \mathbf{P}]^T$ and $\mathbf{F} = [\mathbf{F}_1, \mathbf{F}_2]^T$. In this section, we use a particular kinematics proposed in [15]-[16], even if our models are not exactly similar. Indeed, the kinematics will allow us in future to develop a new experimental protocol for measuring various hydrodynamic parameters of a fin.

4.1 Dynamic response to the fin

To better define a reasonable perfomance of the fin, we take the total expression of the excitation force $\mathbf{F}(t)$ resulting from (6). We then obtain the different response curves where the end $x = 0$ is constrained to a combined translational and rotation motions.

4.1.1 Oriented fibers : $0°/90°/0°/90°/0°$

As a recall, fibers of each layer are arranged alternately along the two directions orthogonal axis **x** and **y** of the mean plane of the fin. For this first fin, the first layer is oriented along **x**. The length of each layer is not the same. Lengths of layers are respectively $\ell := \ell_1 = 0.8[m]$, $\ell_2 = 0.6[m]$, $\ell_3 = 0.5[m]$, $\ell_4 = 0.4[m]$, and $\ell_5 = 0.3[m]$. The total thickness of the fin is maintained constant $e = 5.8[mm]$, and it is not depending on the number of layers.

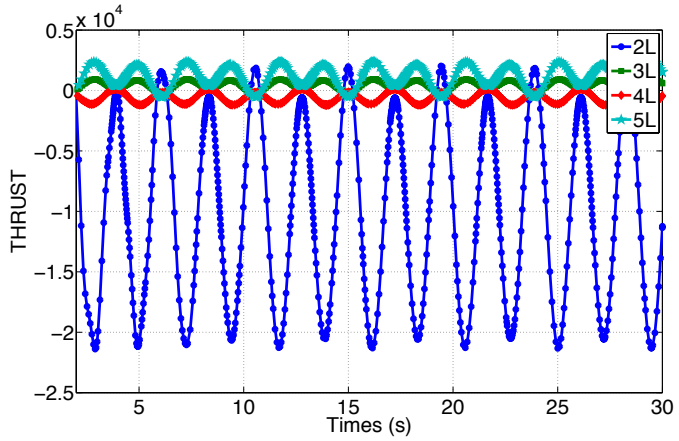

Figure 3: Thrust force $[N]$ during the course of time $[s]$ for the $2L$, $3L$, $4L$, and $5L$ models.

The magnitude of thrust force induced by the two-layers fin is greater than the other fins, although its value is mosty negative. Remind that the eigenfrequency of this fin is the lowest. This nevertheless seems abnormal and requires further close analysis. The behaviours of the other three fins are quite similar.

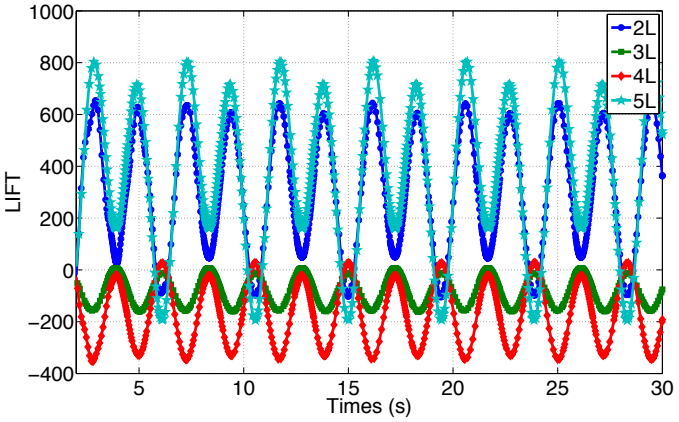

Figure 4: Lift force $[N]$ during the course of time $[s]$ for the $2L$, $3L$, $4L$, and $5L$ models.

We remark that the lift force for the two-layers and the five-layers fins behaves similarly (they are mostly positive), whereas the three and four-layers are quite comparable (they are mostly negative). Magnitude of lift force is greater for the two-layers and the five-layers fins. By the way, they are mostly positive.

The moment magnitude is lowest for the two-layers models, compared to the other fins. Again the two- and five-layers fins have similar behaviour (positive moment), although with

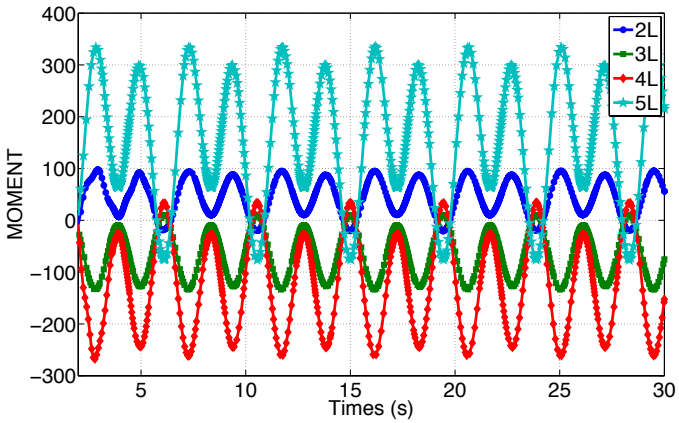

Figure 5: Moment $[m\ N]$ during the course of time $[s]$ for the $2L$, $3L$, $4L$, and $5L$ models.

different magnitude; whereas the three- and four-layers fins have negative moment.

4.1.2 Oriented fibers : $90°/0°/90°/0°/90°$

Recall also that fibers of each layer are arranged alternately along the two directions orthogonal axis **x** and **y** of the mean plane of the fin. However for this second fin, the first layer is oriented along **y**. The length of each layer is not the same. Lengths of layers are respectively $\ell := \ell_1 = 0.8[m]$, $\ell_2 = 0.6[m]$, $\ell_3 = 0.5[m]$, $\ell_4 = 0.4[m]$, and $\ell_5 = 0.3[m]$. The total thickness of the fin is maintained constant $e = 5.8[mm]$, and it is not depending on the number of layers.

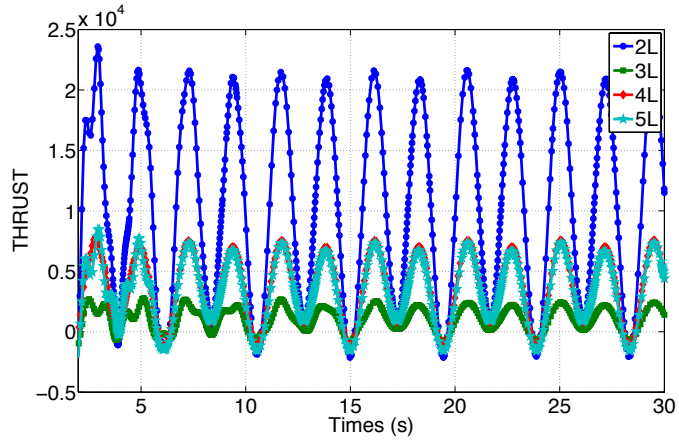

Figure 6: Thrust force $[N]$ during the course of time $[s]$ for the $2L$, $3L$, $4L$, and $5L$ models.

Again, the magnitude of thrust force induced by the two-layers fin is greater than the other fins, although its value is mosty now positive. Remind also that the eigenfrequency of this fin is the lowest. The behaviours of the other three fins are quite similar, with a positive thrust force for all of them (Figure 6).

The four-layers fin present the lowest magnitude for the lift force (mostly negative values), whereas the three-layers fin has the greatest amplitude. The other three models have positive lift force (Figure 7).

The five-layers fin induces very low moment magnitude compared to the other fins. Again

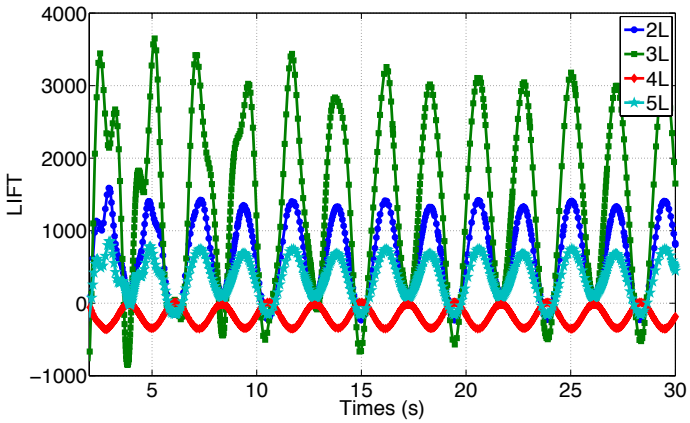

Figure 7: Lift force $[N]$ during the course of time $[s]$ for the $2L$, $3L$, $4L$, and $5L$ models.

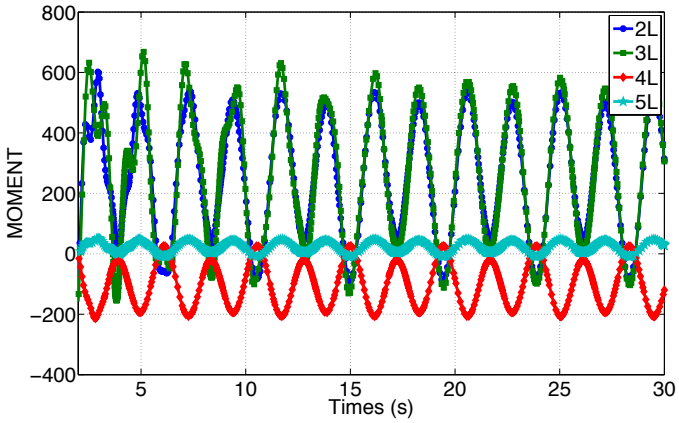

Figure 8: Moment $[m\ N]$ during the course of time $[s]$ for the $2L$, $3L$, $4L$, and $5L$ models.

the four-layers fin has mostly negative moment (Figure 8). Such is not the case for the other models.

Again comparing the two types of multi-layers fins, we may draw some remarks. The two-layers model always gives a greater thrust than the other models. It should be however pointed out that the fibers arrangement may induce negative or positive thrust for this fin. If we eliminate this case, we may see that the five-layers fin gives the best performance.

In a general manner, the three-layers fin seems to give a better compromise. Indeed, its thrust remains positive all the time, while its lift has negative value and nevertheless less of lower importance than other fins. The moment magnitude associated to the three-layers model is also the lowest. In sum, it is then shown that by varying some physical parameters, we can significantly reduce or increase hydrodynamic quantities, such as the thrust, the moment, and the lift.

4.1.3 Water pressure for fin with Oriented fibers : $0°/90°/0°/90°/0°$

To see how the overall response of the coupled system evolves, we display in the figures below (Figure 9) and at different times $t = 2, 4, 6, 8\ [s]$ the pressure field within water, and the iso-acceleration lines. We also display the deformed shapes of the fin (first layer parallel

to $\mathbf{x}$) at the associated times. The present model uses an acoustic model of the water, and

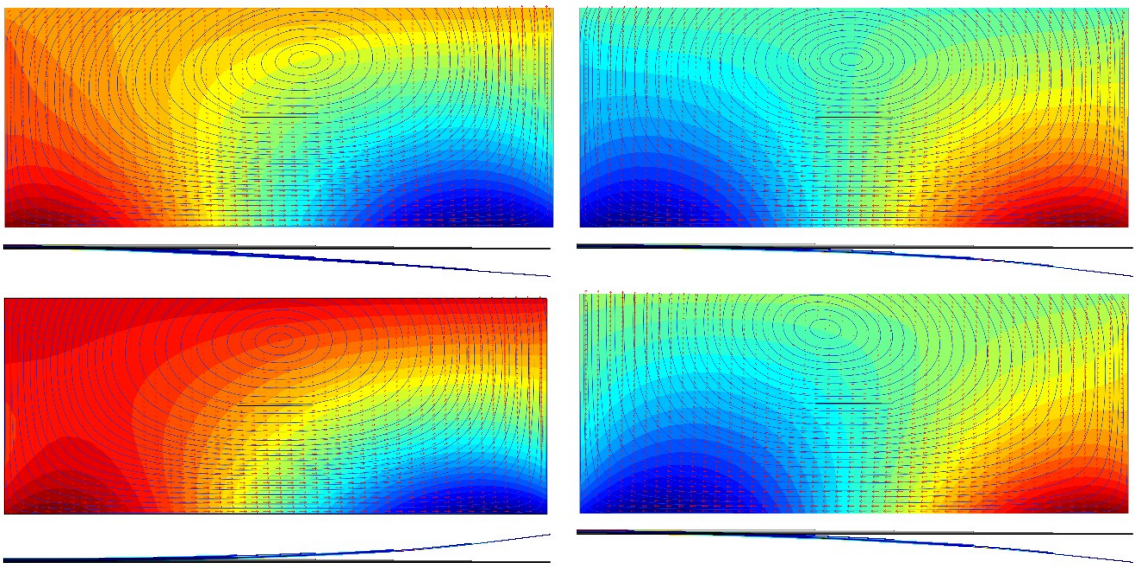

Figure 9: Pressure contour plot $p(\mathbf{x}, t)$, iso-acceleration lines, and associated deformed shapes of the five-layers fin, at different times $t = 2, 4, 6, 8\ [s]$. Remind that the fundamental frequency of this fin is $f_1 = 2.77\ [Hz]$, and the excitation frequency $f_{exc} = 0.225\ [Hz]$. The fin is displayed in the middle region of the pool.

neglects the viscosity, although the thrust production is thought to be strongly correlated with the formation and shedding of leading edge vortices. In a viscous situation, the wake formed behind the fin is affected by the interaction of the leading edge vortex with the fin and with the training vortex. This could captured in our model. In the present study, the evolution of the field pressure $p(\mathbf{x}, t)$ in the course of time shows the influence of the swimming pool dimensions on the result. Accuracy of results may be improved by considering much larger dimensions of the pool.

5 CONCLUDING REMARKS

A parametric analysis of eigenfrequencies of multilayers composite fin has been done by considering the influence of the surrounding water. The fluid flow, and more precisely the evolution of water pressure around a 2D deformable fin, and the deformation of the fin itself in a steady motion due to a harmonic heaving and pitching motions, have been simulated by accounting the mutual interaction of the water and the fin. From the present results, we may draw some concluding remarks.

- The presence of layers provides some flexibility for the fin design as indicated by the results of modal analysis. The first mode is bending type, which justifies the use of models proposed in [11].

- Fins with anisotropic material structures allow to develop a method of layers parametrization to improve performance. It is quite possible now to bring special attention to the structure of the layers, and types of constituent materials thereof.

- The present study points out the sensitivity of the dynamic behavior of the fin with respect to the constitute materials, and also the influence of the boundary conditions for the fluid

domain. Indeed, the presence of rigid walls alters significantly the eigenmodes and frequencies of the coupled system. Accordingly, the dynamic behavior of a swimmer may depend on this location at each time in the pool.

- Finally, to obtain a better thrust, the fin has to be elastic at least in rotation. The amplitude of the vertical translation must be controlled to avoid a too great lift, which may lead to an expenditure of extra energy of the swimmer to remain at a constant depth. The use of multilayer fins allows to control the non desirable excessive variation of lift.

Extension of the present study to 3D fins together with viscous fluid is ongoing.

Acknowledgments.

B.M. was partially supported by the Breier Fin Company, France (CIFRE grants).

REFERENCES

[1] I. Akhtar, R. Mittal, G. V. Lauder and E. Drucker. Hydrodynamic of biologically inspired tandem flapping foil configuration. *Theor. Comput. Fluid Dyn.*, 21, 155-170, 2007.

[2] N. Bideau, B. Mahiou, L. Monier, B. Bideau, G. Nicolas, F. Razafimahery, L. Rakotomanana. Dynamique couplée 2D d'un modèle de palme. *Proceedings, 4èmes journées spécialisées de Natation*, p. 119-120, 27-28 mai 2008, Lille.

[3] A. El-Baroudi, F. Razamahery, N. Bideau, L. Rakotomanana. Inuence of fluid-structure interaction in biomechanics : Application to parametric modal analysis and dynamics of the aorta under a shock, *International Journal in Biomedical Engineering and Technology*, To appear, 2011.

[4] T.Y. Hou, V.G. Stredie, T.Y. Wu. Mathematical modeling and simulation of aquatic and aerial animal locomotion. *Journal of Computational Physics*, 225, 1603-1631, 2007.

[5] W-R. Hu. A numerical study on mechanism of S-Starts of Northern Pike (Esox Lucius). *Journal of Hydrodynamics*, Ser. B, 19(2), 135-142, 2007.

[6] W. Kowalczyk and A. Delgado. Simulation of Fluid Flow in a Chanel Induced by Three Types of Fin-Like Motion. *Journal of Bionic Engineering*, 4, 165-176, 2007.

[7] M. A. Luersen, R. Le Riche. Adapting ply drop positions for compensating fabric changes - Applications to swimming monofins. *Finite Elements in Analysis and Design*, 46, 930-935, 2010.

[8] M. A. Luersen, R. Le Riche, D. Lemosse and O. Le Maître. A computationally efficient approach to swimming monofin optimization. *Struct. Multidisc. Optim.*, 31, 488-496, 2006.

[9] M. Koch, G. Gouvernet, P. Chavet, C. Barla, A. Sabo. Muscle activity during fin swimming. *Procedia Engineering*, 2, 3029-3034, 2010.

[10] J.-M. Miao and M.-H. Ho. Effects of flexure on aerodynamic propulsive efficiency of flapping flexible. *Journal of Fluids and Structures*, 22, 401-419, 2006.

[11] J. C. Mollendorf, J. D. Felske and S. Samimy. A Fluid/Solide Model for Predicting Slender Body Deflection in a Moving Fluid. *Transactions of ASME.*, 346, Vol. 70, May 2003.

[12] G. Nicolas, B. Bideau, B. Colobert and E. Berton. How are Strouhal number, drag, and efficiency adjusted in high level underwater monofin-swimming ? *Human Movement Science*, 26, 426-442, 2007.

[13] G. Pedro, A. Suleman and N. Djilali. A numerical study of the propulsive efficiency of a flapping hydrofoil. *International Journal for Numerical Methods in Fluids*, 42, 493-526, 2003.

[14] L.R. Rakotomanana. *Eléments de dynamique des solides et structures déformables*, Presses Polytechniques et Universitaires Romandes, Lausanne, 2009.

[15] D. A. Read, F. S. Hover and M. S. Triantafyllou. Forces on oscillating foils for propulsion and maneuvering. *Journal of Fluids and Structures*, 17, 163-183, 2003.

[16] S. Shin, S. Y. Bae, I. C. Kim and Y. J. Kim. Effects of flexibility on propulsive force acting on a heaving foil. *Ocean Engineering*, 36, 285-294, 2009.

[17] Schouveiler L., Hover F. S., Triantafyllou M.S. Peformance of flapping foil propulsion. *Journal of Fluids and Structures*, 20, 049-959, 2005.

[18] Y. Yadykin, V. Tenetov and D. Levin. The added mass of a flexible plate oscillating in a fluid. *Journal of Fluids and Structures*, 17, 115-123, 2003.

[19] C. Zhang, L-X. Zhuang and X-Y. Lu. Analysis for hydrodynamics for two-dimensional flow around waving plates. *Journal of Hydrodynamics*, Ser. B, 19(1), 18-22, 2007.